Asymmetric Structure of the Purple Membrane

Abstract. *There is both functional and structural evidence that bacteriorhodopsin is oriented asymmetrically across the purple membrane of* Halobacterium halobium. *To assess the degree of asymmetry, the x-ray diffraction data from the membrane have been analyzed for possible electron-density profiles. A recent theory predicts that only a limited number of profiles are consistent with the continuous diffraction data, and two possible profiles have been found. Both profiles indicate that the protein molecules span a lipid bilayer in the membrane. Both profiles are asymmetric; there are more lipid molecules in one half of the membrane than in the other, and the bacteriorhodopsin molecule shows a slight complementary asymmetry.*

The purple membrane from *Halobacterium halobium* contains a light-driven pump, bacteriorhodopsin (*1*), which spans the membrane. There is both structural and functional evidence that this molecule is oriented in the membrane; that is, there is a structural asymmetry (*1–3*). We have therefore taken up the problem of computing an accurate asymmetric electron-density profile for the membrane.

A theory was developed recently by one of us (*4*) to use the diffuse low-angle x-ray diffraction from an asymmetric membrane in order to calculate possible profiles. A formula was given for calculating one profile, and it was shown that in principle all other possible profiles can be derived from the one. A striking conclusion of the theory is that only a limited number of profiles is consistent with the data from the purple membrane.

We have calculated one possible profile by using the theory. Because we found it difficult to carry out the method proposed for calculating other possible profiles, we have also used an alternative approach. Using the alternative method, we have found two profiles which are consistent with the diffraction from the purple membrane; one of these is the same as the profile calculated by direct application of the theory. To our knowledge, this is the first time an exact membrane profile has been calculated from diffuse intensity data alone.

In general, both the modulus of the Fourier transform $|F|$ and the phase angle ϕ are needed in order to calculate a membrane profile from given diffraction data through the inverse Fourier transformation. Since the corrected profile diffraction from the purple membrane (*2, 3*) provides the curve of $|F|$, the problem is to determine the curve of ϕ in the range where $|F|$ is observed. In fact, as Sayre (*5*) has pointed out, it is sufficient to determine values for ϕ at a number of regularly spaced points.

Our working method was to sample the observed curve of $|F|^2$ (*2, 3*) at a few regularly spaced points and take the square roots, and then to assume sets of values for the corresponding phase angles in order to calculate Fourier transforms. The calculation of a continuous transform F is based on Shannon's sampling theorem, as proposed by Sayre (*5*). Good agreement of the calculated $|F|^2$ with the observed curve means the set of phase angles is acceptable, while poor agreement means the set is unacceptable. There may, of course, be more than one acceptable set of phase angles.

We began by sampling at Bragg spacings of 50 Å/h, where $h = \pm1, \pm2, \ldots$; that is, as though the membranes were in a stack with one membrane every 50 Å. The 50-Å distance ($\equiv D$) was chosen since the periodicity in a stack of the dried membranes is about 50 Å (*2, 3, 6*) and since just two points to either side of the origin cover the range of observation. Values of $|F_h|^2$ for $h \geq 3$ were all taken as zero because the profile diffraction is very weak beyond 0.06 Å^{-1} (*2, 3*).

We applied the same sampling theorem to obtain a value at the origin, $|F_0|^2$ (*4*). The observed curve was sampled at spacings of 100 Å/h, h = 1 to 5. The sampled $|F_h|^2$ values, together with an assumed value for $|F_0|^2$, are sufficient to calculate the continuous curve of $|F|^2$ without computing F first (*5*). An initial value for $|F_0|^2$ was found by trying different values until we had the best fit to the observed curve in the intervals between sampling points.

We then chose sets of the ϕ_h in order to calculate F curves. The phase angle at the origin, ϕ_0, was chosen as zero since F_0 needs to be real and positive—real because F_0 is real in general, and positive because the average electron density of the purple membrane is considerably greater than the average value for the surrounding water (*2, 3*). The other two phase angles, ϕ_1 and ϕ_2, were varied systematically in the range from $-\pi$ to π, which covers all possibilities. In practice the phase angle ϕ_1 can be restricted to

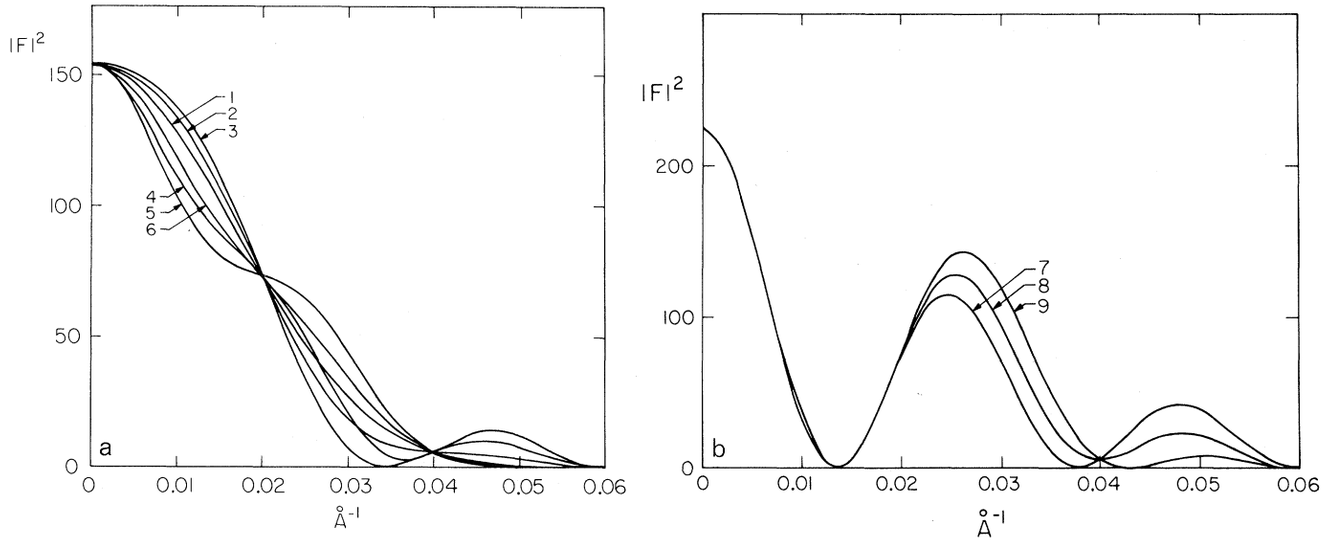

Fig. 1. Squared Fourier transforms calculated by using the Shannon sampling theorem, as proposed by Sayre (*5*). The observed profile diffraction was sampled at the points corresponding to D = 50 Å. The assumed phase angles (ϕ_0, ϕ_1, ϕ_2) are in radians. (a) Curve 1 (0, 0, 0); curve 2 (0, 0, π/2); curve 3 (0, 0, π); curve 4 (0, π/2, 0); curve 5 (0, π/2, π/2); and curve 6 (0, π/2, π). The initial value of F_0 has been used (see text). (b) Curve 7 (0, π, 0); curve 8 (0, π, π/2); and curve 9 (0, π, π). The refined value for F_0 has been used (see text).

positive values since negative values correspond simply to turning the membrane over; values of $n\pi/8$ were tested, where $n = 0, 1, \ldots, 8$. For each value of ϕ_1, ϕ_2 was given the values $n\pi/8$, $n = 0, \pm1, \pm2, \ldots, \pm8$. Since $|F_{-h}| = |F_h|$ and since $\phi_{-h} = -\phi_h$, three values of $|F_h|$ from the observed curve ($h = 0$, 1, and 2) and a set of values for the corresponding ϕ_h are sufficient to calculate a continuous Fourier transform.

The continuous real (F_R) and imaginary (F_I) parts of F were calculated, and the squared modulus, $|F|^2 = F_R^2 + F_I^2$, was then calculated in each case. Some of these curves are shown in Fig. 1. The results in Fig. 1 show that the form of the curve depends strongly on the phase angles chosen. Thus, we have a powerful method for testing possible phase angles.

We found that most of the calculated curves of $|F|^2$ were quite different from the observed diffraction (see Fig. 2a). The formula for calculating the continuous transform (*5*) ensures that the calculated curves all intersect the observed curve at the sampling points. However, in between these nodal points the calculated curves in Fig. 1 diverge widely, and the agreement with observation is very bad in most cases. As illustrated in Fig. 1a, for ϕ_1 equal to 0 or $\pi/2$ and ϕ_2 equal to any of the above values, there was at best only a slight inflection near 0.013 Å^{-1}, in contrast to the near-zero minimum observed there (Fig. 2a). Only when ϕ_1 was close to π ($\phi_1 > 7\pi/8$) did the calculated curves resemble the observed data. Some curves having $\phi_1 = \pi$ are shown in Fig. 1b; the closest resemblance to observation occurs for $\phi_2 = \pi/2$ (and hence also for $\phi_2 = -\pi/2$). Our results therefore established that ϕ_1 must be close to π. At the same time, ϕ_1 cannot be exactly π since then the predicted minimum at 0.013 Å^{-1} was always too close to zero (Fig. 1b). Accordingly, the ϕ_h were refined by trial and error in the ranges $\phi_1 \simeq \pi$ and $\phi_2 \simeq \pm\pi/2$.

Two distinct sets of the ϕ_h were found to give $|F|^2$ curves (not shown) which were identical to each other and which had the general form of the observed diffraction—that is, the highest peak at the origin and two subsidiary peaks to either side (Fig. 2a). However, it was not possible to match the observed Bragg spacings of the peaks and of the minima; rather, in the calculated curves the Bragg spacings were shifted slightly but systematically to smaller values. This result was taken to mean that the 50-Å stacking distance was too small. (It suggests to us that at this distance there may be some interdigitation of molecules in neighboring membranes.) We therefore chose the somewhat larger stacking distance of 67 Å, which allowed us to cover the range of the observed diffraction with three sampling points to either side of the origin. Values of $|F_h|^2$ for $h \geq 4$ were taken as zero.

Values of the $|F_h|^2$ were obtained from the observed diffraction for $D = 67$ Å, and the square roots were calculated. Two sets of starting values for the ϕ_h were obtained from the two best-fit Fourier transforms above and then refined as before. Once again, two distinct sets of the ϕ_h were found to give identical squared Fourier transforms (Fig. 2a). Both the calculated transforms in Fig. 2a reproduce the Bragg spacings and heights of the peaks and minima in the observed curve to a good agreement. The two membrane profiles shown in Fig. 3 were then calculated by sampling the observed diffraction and the two phase-angle curves (Fig. 2b) at Bragg spacings of 100 Å/h, $h = 1$ to 5. The profile in Fig. 3b is identical to the one calculated previously by the direct method in (*4*). We note that the value of F_0 was refined in order to locate the first minimum correctly at 0.013 Å^{-1}.

Assuming, as appears to us to be the case, that the two profiles in Fig. 3 are the only ones (*7*) consistent with the observed diffraction (*2, 3*), what they have in common will necessarily be characteristic of the purple membrane. Both curves include two narrow peaks centered 40 Å apart. The diffraction from the extracted lipids dispersed in water indicates that they form a bilayer with the layers of headgroups centered 40 Å apart (*2, 3*), and the calculated bilayer profile (Fig. 3) shows the expected peaks. The two narrow peaks in either of the membrane profiles in Fig. 3, a or b, therefore are identified with the lipid headgroups in the purple membrane. The alternative interpretation that part of the bacteriorhodopsin molecule accounts for one or both of the high narrow peaks in Fig. 3, a or b, appears inconsistent with the electron microscopic (EM) structure (see

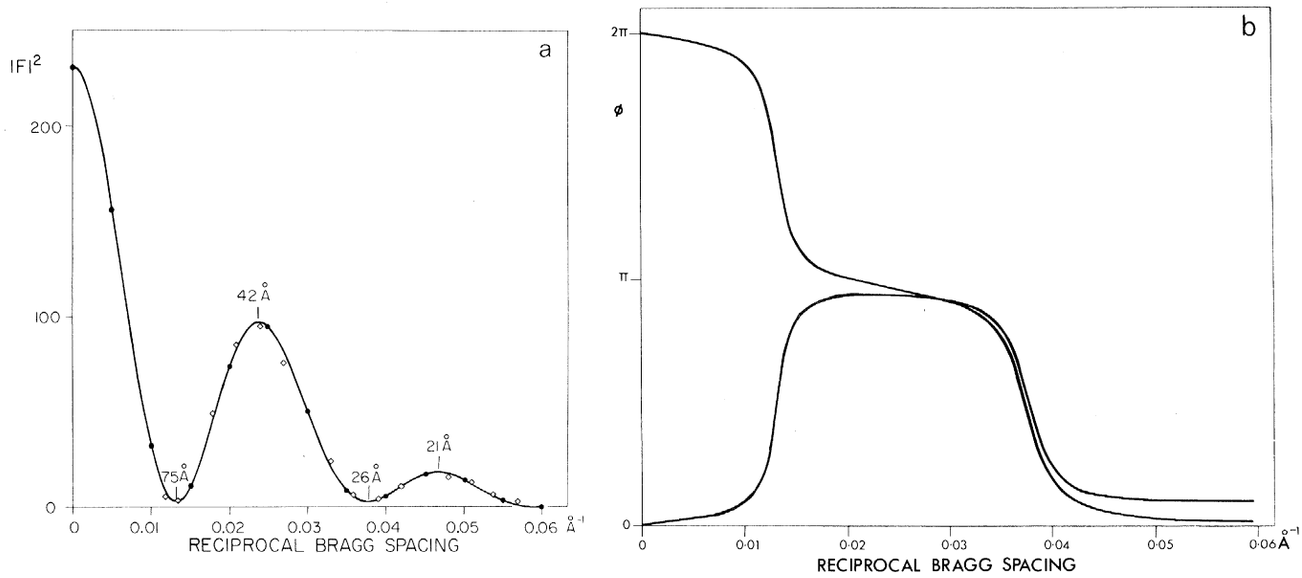

Fig. 2. (a) The two calculated Fourier transforms. The sampling periodicity was $D = 67$ Å, and the refined value of F_0 has been used. The two sets of phase angles were derived as described in the text. (—) Phase angles (ϕ_0, ϕ_1, ϕ_2, ϕ_3) in radians are (0, 0.828π, 0.910π, 0.126π). (•) Phase angles in radians are (0, -0.870π, 0.910π, 0.067π). (◇) Observed profile diffraction after correction for disorientation [data are from (*2, 3*)]. (b) Corresponding curves of the phase angle ϕ.

below). We conclude that there are substantial amounts of lipid on both sides of the membrane. Since the total amount of lipid is hardly enough to form an unbroken monolayer in the membrane (*2, 3*), it follows that the bacteriorhodopsin molecules span the membrane bilayer.

The two profiles are also similar in what they imply for the protein. The region near the center is considerably higher in either profile than in the profile of the extracted lipids after the headgroup peaks are scaled in the respective profiles. This observation confirms that there are large amounts of protein in the core of the membrane. We can also say something about how the protein is distributed.

Figure 3b shows different levels at ± 5 Å from the center, with the higher level at −5 Å. If the bacteriorhodopsin molecule has a fairly uniform electron density, the higher level at −5 Å indicates that more than half of the bulk of the molecule is located on the left side. Assuming that the lipids pack uniformly, there would therefore be room for less than half of the lipid molecules on that side. This arrangement accordingly will account for the smaller headgroup peak on the left side. Thus, we are able to make a consistent interpretation of this profile.

Figure 3a similarly shows a higher level at −5 Å than at +5 Å. This observation indicates that more than half of the membrane protein is on the left side, and there would be room for less than half of the lipid molecules on this side. The height of the right headgroup peak above the level at +5 Å is greater than that of the left headgroup peak above the level at −5 Å, suggesting that more than half the lipid is indeed on the right side. Thus, the two profiles lead to similar and reasonable conclusions about the distribution of lipid and protein in the membrane.

To further examine the two different phasings, we have calculated the curve for ϕ in each case. The two curves in Fig. 2b have similar values around the reciprocal spacings of the two subsidiary peaks in $|F|^2$: close to π across the peak at 42 Å and close to zero (equivalent to 2 π) across the peak at 21 Å. They differ mainly in whether they pass through $\pi/2$ or $3\pi/2$ near the minimum at 75 Å. As noted above, however, changing the sign of ϕ at every point corresponds simply to turning the membrane over. In this way, the two curves can be made nearly coincident out to 0.03 Å^{-1}. Thus at lower resolution the two asymmetric profiles are nearly identical. The dissimilarities between the two profiles in Fig. 3 in fact depend mainly on the phasing in an interval around 0.04 Å^{-1}. As yet we have no way to decide which of the two profiles in Fig. 3 is correct.

We are obliged to state an important caveat: both profiles in Fig. 3 may be inaccurate because of possible systematic errors in the intensity data. It has been noted that the diffraction minima observed at 75 and 26 Å may be artificially high (*2, 3*). There are several independent effects which could give too high a value, and none would give too low a value. The two profiles in Fig. 3 therefore may overstate the asymmetry. The unique symmetric profile toward which the two profiles tend as the two minima go toward zero is shown in figure 3 of Blaurock and Stoeckenius (*2*).

It remains to correlate our results with the EM study by Henderson and Unwin (*8*). We first note that our results are not redundant with the EM results. The EM observations could not be made within a cone centered on the profile axis and having a half-angle of 33° (*8*). However, much of the intensity within this region, including the profile diffraction, can be related directly to the lipid bilayer structure of the membrane (*2, 3*). Thus, while the shape and orientation of the bacteriorhodopsin molecules found by EM allow for patches of lipid bilayer, the lipid molecules were not seen by EM. The x-ray data therefore remain the most direct test of whether the bilayer is present. Our results here, together with previous observations (*2, 3*), establish the lipid bilayer beyond reasonable doubt.

The bacteriorhodopsin molecule was found by EM to consist largely of a cluster of seven rods of α-helix nearly as long as the membrane is thick (*8*), and the molecule therefore appears to have a nearly uniform cross-sectional area. Given this result and assuming that the protein is located symmetrically, we expect nearly equal amounts of lipid on the two sides of the membrane. Thus the two x-ray profiles may be overstating the asymmetry of the membrane profile. However, the omission of the EM data in the 33° cone may have biased the electron diffraction results toward a symmetric structure. The interesting question of the precise degree of asymmetry of the purple membrane therefore remains unanswered.

In summary, our results confirm the earlier theoretical conclusion that only a limited number of phasings are consistent with the continuous diffraction data from the purple membrane. We find two profiles consistent with the data out to 0.06 Å^{-1}. Both profiles are asymmetric, as expected from other structural and functional observations on the purple

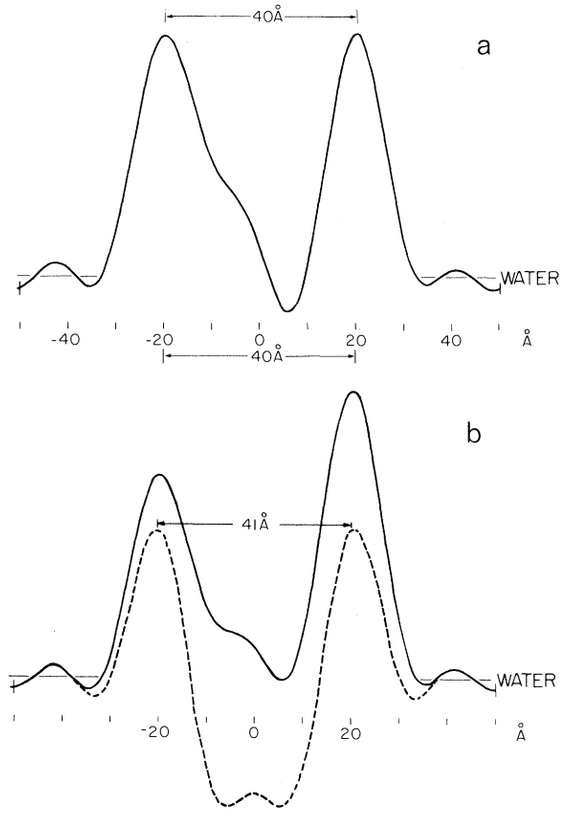

Fig. 3. Calculated membrane profiles. The profile of the extracted lipids (dashed line) is superimposed in (b). The lipid profile is to the same resolution as the membrane profile, but these two profiles are not to scale vertically.

membrane. Both profiles indicate that the membrane lipids are in the bilayer arrangement. At the same time, the average level near the center of either membrane profile is considerably higher than the level near the center of the extracted-lipids profile. This observation confirms that the bacteriorhodopsin molecules extend through the bilayer. We also find that the smallest stacking distances observed, ~ 50 Å, are too small to allow a good fit of calculated to observed profile diffraction. This result appears to mean that the membrane in suspension is thicker than 50 Å; for example, the bacteriorhodopsin molecules may project out beyond the lipid bilayer.

ALLEN E. BLAUROCK*
MRC Cell Biophysics Unit, Biophysics Department, King's College, London WC2B 5RL, England
GLEN I. KING†
Cardiovascular Research Institute, University of California, San Francisco 94143

References and Notes

1. D. Oesterhelt and W. Stoeckenius, *Proc. Natl. Acad. Sci. U.S.A.* **70**, 2853 (1973).
2. A. E. Blaurock and W. Stoeckenius, *Nature (London) New Biol.* **233**, 152 (1971).
3. A. E. Blaurock, *J. Mol. Biol.* **93**, 139 (1975).
4. G. I. King, *Acta Crystallogr. Sect. A* **31**, 130 (1975).
5. D. Sayre, *Acta Crystallogr.* **5**, 843 (1952).
6. R. Henderson, *J. Mol. Biol.* **93**, 123 (1975).
7. The number of possible profiles, and these profiles themselves, can in principle be calculated as indicated in (*4*). However, the attempt to calculate profiles other than the one principal solution has so far been unsuccessful.
8. R. Henderson and P. N. T. Unwin, *Nature (London)* **257**, 28 (1975).
9. G.I.K. thanks J. Woodard for help with computer calculations and A.E.B. thanks A. Kernaghan for drafting figures. Both authors thank R. Henderson and N. Unwin for the personal communication that the α-helices in bacteriorhodopsin fan out toward one side of the membrane. As a result, there may be room for one less lipid molecule, per bacteriorhodopsin, on the corresponding side of the membrane. Both effects will help to account for the asymmetry we have found. Supported by Public Health Service NEI special fellowship F03 EY 50, 584 (A.E.B.) and program project grant HL-06285 (G.I.K.). Contribution No. 5482 from California Institute of Technology.
* Present address: Division of Chemistry and Chemical Engineering, California Institute of Technology, Pasadena 91125.
† Send reprint requests to G.I.K.

7 October 1976; revised 21 December 1976

The Earth as a Seismic Absorption Band

Abstract. *Attenuation of seismic waves indicates that the earth is not perfectly elastic. Dispersion accompanying absorption gives frequency-dependent "elastic" moduli, a fact that must be taken into account when inverting seismic data. Normal mode data are reinverted after correcting for absorption. The correction removes the discrepancy between body wave and free oscillation interpretations of earth structure.*

The earth is often assumed to be a perfectly elastic body. One consequence of this assumption is that elastic moduli and seismic velocities do not depend on frequency. Thus, if the assumption is valid, the moduli determined from seismic body waves can be compared directly with surface wave, free oscillation, and ultrasonic laboratory results and used to compute tidal response, Chandler wobble periods, and static deformation of the lithosphere. However, "elastic" waves are nondispersive only at very high and very low frequencies, and ideal elastic behavior is only approached at very low temperatures. The absorption of seismic body waves and the decay of free oscillations indicate that the earth is not a perfectly elastic body. It is well known that dispersion must accompany absorption (*1*) and therefore elastic moduli depend on frequency. The travel times of body waves and the periods of free oscillation are now known to better than 0.1 percent; the effect of dispersion over the seismic frequency band can amount to 1 percent, and it is therefore a nonnegligible effect. Jeffreys (*2*) has long maintained that physical dispersion is important, and some attempts have been made to use the effect to reconcile body wave and surface wave earth models (*3*). Randall (*4*) recently further stressed this point. Liu *et al.* (*5*) calculated the dispersion-absorption for a solid having a spectrum of relaxation mechanisms, and we use their results in this report.

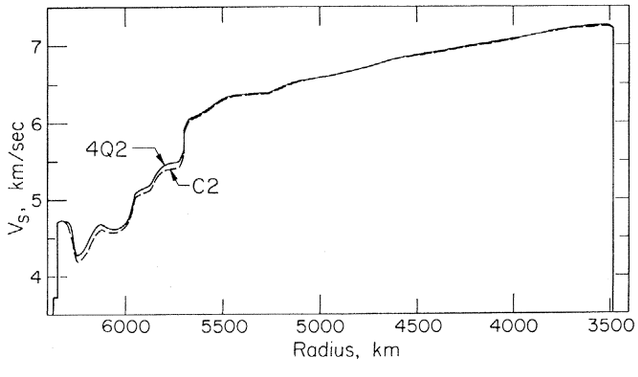

Fig. 1. Shear velocities plotted against radius for model C2, which assumes that the earth is perfectly elastic, and model 4Q2, which is based on the inversion of torsional oscillations data corrected for attenuation.

Relaxation phenomena are most likely to be responsible for seismic absorption (*6, 7*). Relaxation mechanisms include grain boundary effects, partial melting, phase changes, stress-induced atomic reordering, and thermoelasticity. Absorption in a medium with a single characteristic relaxation time, τ, gives rise to the familiar bell-shaped Debye peak centered at a frequency $\omega = \tau^{-1}$. The specific dissipation function, Q^{-1}, and phase velocity satisfy the differential equation for the standard linear solid and can be written (*8, 9*)

$$Q^{-1}(\omega) = 2Q_m^{-1}\omega\tau/(1 + \omega^2\tau^2) \quad (1)$$

$$C^2(\omega) = C_0^2(1 + \omega^2\tau^2C_\infty^2/C_0^2)/[(1 + \omega^2\tau^2)^2 + 2\omega^2\tau^2Q_m^{-1}]^{1/2} \quad (2)$$

The high-frequency, C_∞, and low-frequency, C_0, velocities are related by

$$\frac{C_\infty^2 - C_0^2}{C_0C_\infty} = 2Q_m^{-1}$$

In the equations above, Q_m^{-1} is the peak value of the specific dissipation function at $\omega\tau = 1$. The low- and high-frequency limits of Q^{-1} are, respectively,

$$Q^{-1}(\omega) = 2Q_m^{-1}\omega\tau \quad (3)$$

and

$$Q^{-1}(\omega) = 2Q_m^{-1}(\omega\tau)^{-1} \quad (4)$$

Note that the magnitude of the peak dissipation depends on the total range of velocities. The phase velocity is only constant at high and low frequencies; in these limits Q^{-1} varies as ω or ω^{-1}. Laboratory data on attenuation (*8, 9*) indicate that the absorption peak is generally much broader than given by Eq. 1. This is usually interpreted in terms of a distribution of relaxation times.

The fact that seismic values for Q^{-1} are roughly frequency-independent and are comparable in magnitude to peak attenuation values in polycrystalline oxides and silicates (*10*) suggests that seismic frequencies are in the midst of a broad absorption band. Shear waves reflected from the core (ScS waves) of period 10 to 50 seconds and toroidal oscillations having periods greater than 1000 seconds both sample the entire mantle and have approximately the same Q (*11, 12*). This suggests that Q cannot have the